J|A|C|S
ARTICLES
Published on Web 10/18/2006

Photooxidation of Olefins under Oxygen in Platinum(II) Complex-Loaded Mesoporous Molecular Sieves

Ke Feng,[†] Ren-Yuan Zhang,[‡] Li-Zhu Wu,*[,†] Bo Tu,[‡] Ming-Li Peng,[†] Li-Ping Zhang,[†] Dongyuan Zhao,*[,‡] and Chen-Ho Tung[†]

Contribution from the Laboratory of Supramolecular Photochemistry, Technical Institute of Physics and Chemistry & Graduate University, the Chinese Academy of Sciences, Beijing 100080, People's Republic of China, and Department of Chemistry, Shanghai Key Laboratory of Molecular Catalysis and Innovative Materials and Advanced Materials Laboratory, Fudan University, Shanghai 200433, People's Republic of China

Received July 14, 2006; E-mail: lzwu@mail.ipc.ac.cn; dyzhao@fudan.edu.cn

Abstract: Cyclometalated platinum(II) complex has been successfully incorporated into the (3-aminopropyl) triethoxysilane-modified channels of ordered mesoporous silica SBA-15 that has large pore hexagonal channels. Studies on the $^1O_2$ generation conclusively demonstrates that the olefins in the nano-channels of SBA-15 can be enriched 8 times higher than those in the homogeneous solution as the diffusion quantum yield of singlet oxygen ($^1O_2$) is assumed to be unit. The platinum(II) complex loaded in the channel of SBA-15 is stable, and the photosensitized oxidation occurs efficiently. No obvious degradation and leaching of photosensitizers is observed even after 10 runs. Only a simple filtration is needed for the recycled use of the expensive noble metal catalysts. This versatile system is a good example of photochemical reactions occurring in the mesoporous silica molecular sieve. SBA-15 not only provides a support for the photosensitizer, but also acts as a nano-reactor to facilitate the photooxidation.

Introduction

Square-planar platinum(II) polypyridyl complexes represent an important class of compounds that possess a rich range of spectroscopic and photophysical properties.[1−10] Some of them have demonstrated promising potentials in various applications, such as optical power limiting,[3] electroluminescence,[4] sensors,[5,6] and multi-electron-transfer processes.[7] In the context of the photochemistry, this kind of complex has appeared at the forefront due to its unique properties of open axial coordination site and strong visible absorptions.[1] Gray took the lead in developing solar chemistry of metal complexes.[8] Eisenberg and our group have shown that the platinum(II) terpyridyl complexes can be employed as photocatalysts to produce H_2 from either aqueous protons in the presence of a sacrificial electron donor or Hantzsch dihydropyridine derivatives.[9] More recently, we have further employed platinum(II) polypyridyl complexes as sensitizers for photooxidation using molecular oxygen,[10] where singlet oxygen ($^1O_2$) was generated upon irradiation of light in visible region. However, these appealing features are outweighted by the relatively high costs and low stability in solution, which make their synthetic application impractical. Thus, seeking new photosensitizers or photosensitized systems

[†] Technical Institute of Physics and Chemistry, the Chinese Academy of Sciences.

[‡] Fudan University.

(1) (a) Houlding, V. H.; Miskowski, V. M. *Coord. Chem. Rev.* **1991**, *111*, 145−152. (b) Lai, S.-W.; Che, C.-M. *Top. Curr. Chem.* **2004**, *241*, 27−63. (c) Chan, C.-W.; Cheung, L.-K.; Che, C.-M. *Coord. Chem. Rev.* **1994**, *132*, 87−97. (d) McMillin, D. R.; Moore, J. J. *Coord. Chem. Rev.* **2002**, *229*, 113−121. (e) Yam, V. W.-W. *Acc. Chem. Res.* **2002**, *35*, 555−563.

(2) (a) Connick, W. B.; Miskowski, V. M.; Houlding, V. H.; Gray, H. B. *Inorg. Chem.* **2000**, *39*, 2585−2592. (b) Whittle, C. E.; Weinstein, J. A.; George, M. W.; Schanze, K. S. *Inorg. Chem.* **2001**, *40*, 4053−4062. (c) Liu, Y.; Jiang, S.; Glusac, K.; Powell, D. H.; Anderson, D. F.; Schanze, K. S. *J. Am. Chem. Soc.* **2002**, *124*, 12412−12413. (d) Yang, Q.-Z.; Wu, L.-Z.; Wu, Z.-X.; Zhang, L.-P.; Tung, C.-H. *Inorg. Chem.* **2002**, *41*, 5653−5655.

(3) (a) Sun, W.; Wu, Z.-X.; Yang, Q.-Z.; Wu, L.-Z.; Tung, C.-H. *Appl. Phys. Lett.* **2003**, *82*, 850−852. (b) McKay, T. J.; Bolger, J. A.; Staromlynska, J.; Davy, J. R. *J. Chem. Phys.* **1998**, *108*, 5537−5541.

(4) (a) Lu, W.; Mi, B.-X.; Chan, M. C. W.; Hui, Z.; Che, C.-M.; Zhu, N.; Lee, S.-T. *J. Am. Chem. Soc.* **2004**, *126*, 4958−4971. (b) D'Andrade, B. W.; Brooks, J.; Adamovich, V.; Thompson, M. E.; Forrest, S. R. *Adv. Mater.* **2002**, *14*, 1032−1036. (c) Lin, Y.-Y.; Chan, S.-C.; Chan, M. C. W.; Hou, Y.-J.; Zhu, N.; Che, C.-M.; Liu, Y.; Wang, Y. *Chem.-Eur. J.* **2003**, *9*, 1263−1272.

(5) (a) Grove, L. J.; Rennekamp, J. M.; Jude, H.; Connick, W. B. *J. Am. Chem. Soc.* **2004**, *126*, 1594−1595. (b) Wadas, T. J.; Wang, Q.-M.; Kim, Y.-J.; Flaschenreim, C.; Blanton, T. N.; Eisenberg, R. *J. Am. Chem. Soc.* **2004**, *126*, 16841−16849. (c) Yam, V. W.-W.; Wong, K. M.-C.; Zhu, N. *J. Am. Chem. Soc.* **2002**, *124*, 6506−6507. (d) Yam, V. W.-W.; Tang, R. P.-L.; Wong, K. M.-C.; Lu, X.-X.; Cheung, K.-K.; Zhu, N. *Chem.-Eur. J.* **2002**, *8*, 4066−4076. (e) Yang, Q.-Z.; Wu, L.-Z.; Zhang, H.; Chen, B.; Wu, Z.-X.; Zhang, L.-P.; Tung, C.-H. *Inorg. Chem.* **2004**, *43*, 5195−5197. (f) Yang, Q.-Z.; Tong, Q.-X.; Wu, L.-Z.; Wu, L.-Z.; Zhang, L.-P.; Tung, C.-H. *Eur. J. Inorg. Chem.* **2004**, 1948−1954. (g) Siu, P. K. M.; Lai, S.-W.; Lu, W.; Zhu, N.; Che, C.-M. *Eur. J. Inorg. Chem.* **2003**, *15*, 2749−2752. (h) Kui, S. C. F.; Chui, S. S.-Y.; Che, C.-M.; Zhu, N. *J. Am. Chem. Soc.* **2006**, *128*, 8297−8309.

(6) Che, C. M.; Fu, W. F.; Lai, S. W.; Hou, Y. J.; Liu, Y. L. *Chem. Commun.* **2003**, 118−119.

(7) (a) Hissler, M.; McGarrah, J. E.; Connick, W. B.; Geiger, D. K.; Cummings, S. D.; Eisenberg, R. *Coord. Chem. Rev.* **2000**, *208*, 115−137. (b) Wadas, T. J.; Chakraborty, S.; Lachicotte, R. J.; Wang, Q.-M.; Eisenberg, R. *Inorg. Chem.* **2005**, *44*, 2628−2638. (c) Pomestchenko, I. E.; Luman, C. R.; Hissler, M.; Ziessel, R.; Castellano, F. N. *Inorg. Chem.* **2003**, *42*, 1394−1396.

(8) (a) Gray, H. B.; Maverick, A. W. *Science* **1981**, *214*, 1201−1205. (b) Vlcek, A., Jr.; Gray, H. B. *J. Am. Chem. Soc.* **1987**, *109*, 286−287.

(9) (a) Du, P.; Schneider, J.; Jarosz, P.; Eisenberg, R. *J. Am. Chem. Soc.* **2006**, *128*, 7726−7727. (b) Zhang, D.; Wu, L.-Z.; Zhou, L.; Han, X.; Yang, Q.-Z.; Zhang, L.-P.; Tung, C.-H. *J. Am. Chem. Soc.* **2004**, *126*, 3440−3441.

(10) (a) Zhang, D.; Wu, L.-Z.; Yang, Q.-Z.; Li, X.-H.; Zhang, L.-P.; Tung, C.-H. *Org. Lett.* **2003**, *5*, 3221−3224. (b) Li, X.-H.; Wu, L.-Z.; Zhang, L.-P.; Tung, C.-H.; Che, C.-M. *Chem. Commun.* **2001**, *21*, 2280−2281. (c) Yang Y.; Zhang, D.; Wu, L.-Z.; Chen, B.; Zhang, L.-P.; Tung, C.-H. *J. Org. Chem.* **2004**, *69*, 4788−4791.

Scheme 1. Mechanism of $^1O_2$ Photooxidation in Cyclometalated Platinum(II) Complex-Loaded SBA-15 Mesoporous Molecular Sieves

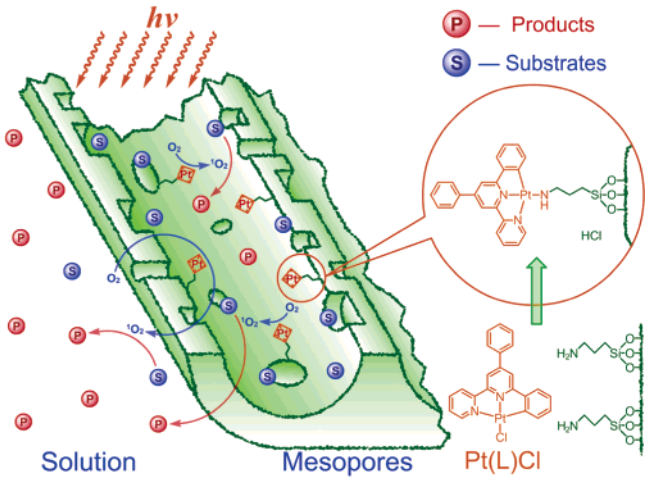

that are capable of inducing high quantum yield of $^1O_2$, and producing cheap and environmental friendly reagent, represents a major target from the synthetic and industrial point of view.

Inspired by the work of Crudden et al., who demonstrated that mercaptopropyl-modified SBA-15 mesoporous materials are remarkable palladium catalysts for coupling reactions,[13] and by Che et al., who immobilized platinum(II) complex into mesoporous silicate MCM-41 to detect solvatochromic response imposed by environmental changes,[6] we envisioned that polypyridyl platinum(II) complexes can be anchored into the channel of mesoporous silica materials, and the photosensitized oxidation may occur in the channel of mesoporous nano-reactor. It has been well established that periodic mesoporous materials possess uniform pore sizes (1.5−40 nm), large surface areas (up to 2000 m^2/g), and tunable structures.[11] This kind of material, without a doubt, contributes one of the most promising candidates for the nano-reactors of large organic molecules.[12] In the present work, we shall report that cyclometalated platinum(II) 4,6-diphenyl-2,2′-bipyridine complex can be successfully immobilized into the nano-channels of the (3-aminopropyl)-triethoxysilane (APTES)-modified mesoporous silica SBA-15, which is an outstanding member in the family of mesoporous materials,[11d,e] and a versatile photooxidation system (Scheme 1) has been established.

Results and Discussion

Immobilization. Complex Pt(L)Cl was prepared by reflux of 4,6-diphenyl-2,2′-bipyridine with K_2PtCl_4 in a mixture of acetonitrile and water.[14] The mesoporous molecular sieves were synthesized via surfactant self-assembly approach.[11] Immobilization of complex Pt(L)Cl into mesoporous molecular sieves was achieved by reacting Pt(L)Cl complex with APTES-modified SBA-15 silica surface, as depicted in Scheme 1. Typically, 10.0 mL of Pt(L)Cl solution (6.25×10^{-2} mg/mL in chloroform) was stirred with 150 mg of APTES-modified SBA-15-b for 12 h. The solid was filtered, and then washed with chloroform more than five times to make sure that there was no liberating Pt(L)Cl adsorbed on the surface of the porous materials. The solid was dried under vacuum condition to afford a slight yellow powder. All of the filtrate and the washing solvent were collected and concentrated to a suitable volume, then in turn to determine the loading level of platinum(II) complex in mesoporous molecular sieves by measuring the absorbance of unloaded Pt(L)Cl concentrations at 440 nm with reference to the Job plot (Supporting Information Figure S1, $(0.91-29.0) \times 10^{-6}$ mol L^{-1} Pt(L)Cl in $CHCl_3$, $R = 0.999$). In this case, the loading ratio to the ploughed amount was 100%, and thus the loading level of Pt(L)Cl was 0.41 wt %.

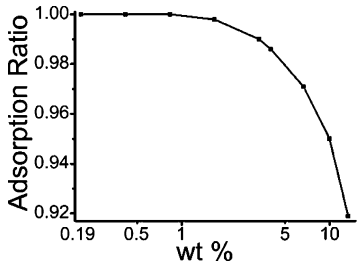

Figure 1. Normalized loading ratio (to the ploughed amount) versus the Pt(L)Cl wt % in SBA-15-b.

Other immobilization experiments were carried out under different ratios of Pt(L)Cl versus APTES-modified SBA-15-b. It was noted that the loading level of Pt(L)Cl can be quantitatively controlled by the initial ratio of Pt(L)Cl versus mesoporous silica matrix, as shown in Figure 1. Pt(L)Cl with various loading levels from 0.21 to 12.3 wt % were obtained for further experimental use.

Comparison of the binding experiments between Pt(L)Cl and *n*-propylamine was performed. Time-dependent UV/vis and emission spectra are shown in Figure 2. In a time scale of 1200 min, the fluorescent intensity decreased in the first 15 min, the peak wavelength decreased from 557 to 555 nm, and then the intensity increased for the rest of the time. The peak wavelength shifted to 548 nm, similar to $[Pt(L)NH_2{}^tBu]ClO_4$ ($\lambda_{max} = 550$ nm in acetonitrile).[6] The changes in the UV−vis and the emission spectra indicate that the binding of Pt(L)Cl and *n*-propylamine takes place.

The diffusion reflectance UV−visible spectroscopy (UV-DRS) of platinum(II) complex-loaded SBA-15 exhibits broad energy absorption bands at the wavelengths of 287, 318, 354, and 402 nm, respectively, which is quite similar to that of Pt(L)(*n*-propylamine)$^+$ in acetonitrile solution (Figure 3). This observation suggests the connection between Pt(L)Cl complex and the amidogen in the channels of APTES-modified SBA-15 molecular sieves. By virtue of coordinative interaction, cyclometalated platinum(II) complex has been anchored into the pore channels of ordered mesoporous silica SBA-15. Such a connection simplifies the synthetic process as compared to covalent-linked systems.

(11) (a) Kresge, C. T.; Leonowicz, M. E.; Roth, W. J.; Vartuli, J. C.; Beck, J. S. *Nature* **1992**, *359*, 710−712. (b) Beck, J. S.; Vartuli, J. C.; Roth, W. J.; Leonowicz, M. E.; Kresge, C. T.; Schmitt, K. D.; Chu, C. T.-W.; Olson, D. H.; Sheppard, E. W.; McCullen, S. B.; Higgins, J. B.; Schlenker, J. L. *J. Am. Chem. Soc.* **1992**, *114*, 10834−10843. (c) Cai, Q.; Luo, Z.; Pang, W.; Fan, Y.; Chen, X.; Cui, F. *Chem. Mater.* **2001**, *13*, 258−263. (d) Zhao, D.; Feng, J.; Huo, Q.; Melosh, N.; Fredrickson, G. H.; Chmelka, B. F.; Stucky, G. D. *Science* **1998**, *279*, 548−552. (e) Zhao, D.; Huo, Q.; Feng, J.; Chmelka, B. F.; Stucky, G. D. *J. Am. Chem. Soc.* **1998**, *120*, 6024−6036.

(12) (a) Jang, J.; Lim, B.; Lee, J.; Hyeon, T. *Chem. Commun.* **2001**, 83−84. (b) Yu, S.; Wang, L.; Chen, B.; Gu, Y.; Li, J.; Ding, H.; Shan, Y. *Chem.-Eur. J.* **2005**, *11*, 3894−3898. (c) Fan, J.; Shui, W.; Yang, P.; Wang, X.; Xu, Y.; Wang, H.; Chen, X.; Zhao, D. *Chem.-Eur. J.* **2005**, *11*, 5391−5396.

(13) Crudden, C. M.; Sateesh, M.; Lewis, R. *J. Am. Chem. Soc.* **2005**, *127*, 10045−10050.

(14) Lai, S. W.; Chan, M. C. W.; Cheung, T. C.; Peng, S. M.; Che, C. M. *Inorg. Chem.* **1999**, *38*, 4046−4055.

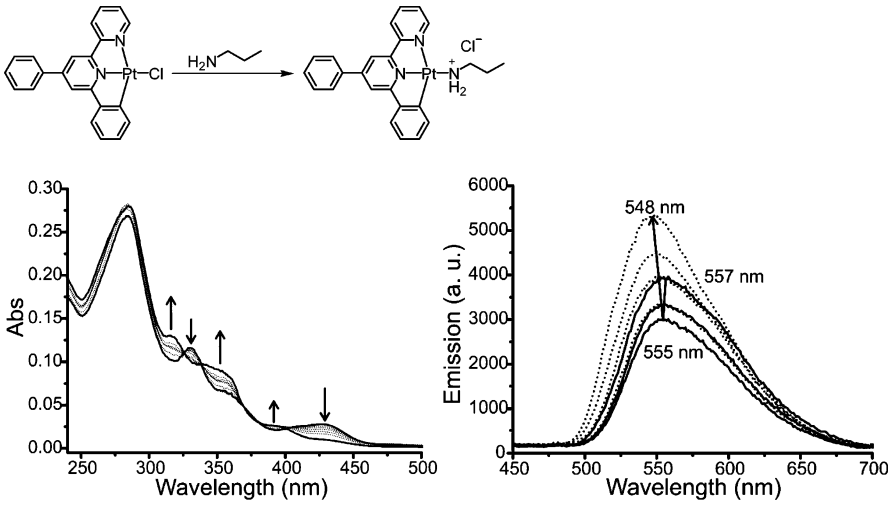

Figure 2. The time-dependent UV/vis and emission spectra of Pt(L)Cl and *n*-propylamine (1:32).

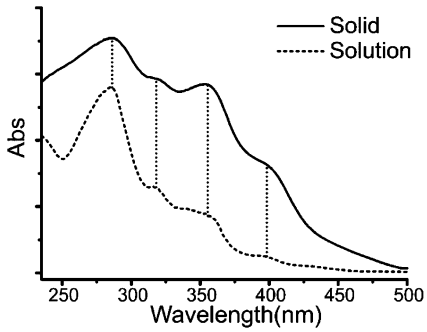

Figure 3. UV-DRS spectra of APTES-modified SBA-15 immobilized with Pt(L)Cl in the solid state and UV/vis spectra of Pt(L)Cl binding with *n*-propylamine in solution.

The luminescence profile of platinum(II) complex-loaded SBA-15 powder shows the emissive band in the range of 500−700 nm with λ_{max} at 547 nm, under the excitation at 360 nm. The lifetime of 3.3 wt % platinum(II) complex-loaded SBA-15 powder was measured to be 1.49 μs (SI Figure S2), which is comparable to that of [Pt(L)NH$_2$^{t}Bu]ClO$_4$ (λ_{max} = 550 nm, τ = 1.0 μs) in acetonitrile solution.[6] With reference to previous spectroscopic work on the cyclometalated platinum(II) complexes,[6,14] the emissive state can be assigned as a typical triplet metal-to-ligand charge-transfer (^{3}MLCT) excited state of platinum(II) complexes.

Singlet Oxygen Production. It is known that the emissive ^{3}MLCT excited states of platinum(II) complexes are responsible for singlet oxygen ($^1O_2$) production.[10] To assess the $^1O_2$ generation ability of the platinum(II) complex-loaded SBA-15 sample, 2,2,6,6-tetramethylpiperidine (TMP) was used as a probe molecule to react with singlet oxygen, yielding stable free radical nitroxide (2,2,6,6-tetramethylpiperidine oxide, TMPO), which can be easily detected by electron spin resonance (ESR) spectroscopy.[15] It is clearly shown in Figure 4 that nitroxide radicals TMPO were generated when oxygen saturated TMP acetonitrile solution was irradiated under the laser beam. The longer the irradiation time is, the stronger the signal intensity will be. Control experiments reveal that light, platinum(II) complex, oxygen, and TMP are all essential for the production

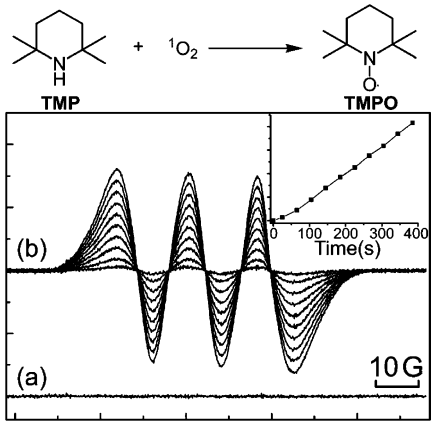

Figure 4. ESR spectra of nitroxide radical generated by irradiation of platinum(II) complex-loaded SBA-15 suspended in an oxygen saturated acetonitrile solution of TMP: (a) in the dark; (b) the sample was continuously scanned for 10 cycles under irradiation; the inset shows the intensity increasing trend of the third peak in a scale of ca. 400 s.

of the ESR signal. Therefore, the emissive ^{3}MLCT excited state of cyclometalated platinum(II) complex in the channel of SBA-15 is believed to operate the energy transfer process with molecular oxygen and thus to generate singlet oxygen ($^1O_2$) efficiently and persistently in this system.

Photooxidation. Photosensitized oxidation was performed at room temperature. A small amount (5 mg) of 0.41 wt % platinum(II) complex-loaded SBA-15 powder used as the photosensitizer was added into the vessel that contains 5 mL of substrates **1** or **3** solution (1.0×10^{-3} mol^{-1} L). The mixture was magnetically stirred in a glass tube and irradiated with a 500 W Hg lamp with oxygen current bubbled in. A quartz jacket with water circulation was used to cool the lamp. A light filter was placed outside the quartz jacket to cut off light below 450 nm and thus guarantee irradiation with visible light. After irradiation, the mixture was centrifuged under 3000 rpm for 15 min, and the upper liquid was separated for further gas chromatograph (GC) detection. As shown in Scheme 2, these two rich electron stilbene derivatives **1** and **3** undergo [2+2] cycloaddition[16] to afford the epoxy intermediates, which quickly

(15) (a) Lion, Y.; Delmelle, M.; Vorst, A. *Nature (London)* **1976**, *263*, 442−443. (b) Moan, J.; Wold, E. *Nature (London)* **1979**, *279*, 450−451. (c) Zang, L. Y.; Frederik, J. G. M. K.; Bibhu, R. M.; Hara, P. M. *Biochem. Mol. Biol. Int.* **1995**, *37*, 283−293.

(16) (a) Tung, C.-H.; Wu, L.-Z.; Zhang, L.-P.; Chen, B. *Acc. Chem. Res.* **2003**, *36*, 39−47. (b) Li, H.-R.; Wu, L.-Z.; Tung, C.-H. *J. Am. Chem. Soc.* **2000**, *122*, 2446−2451. (c) Clennan, E. L.; Pace, A. *Tetrahedron* **2005**, *61*, 6665−6691. (d) Adam, W.; Prein, M. *Acc. Chem. Res.* **1996**, *29*, 275−283.

Scheme 2

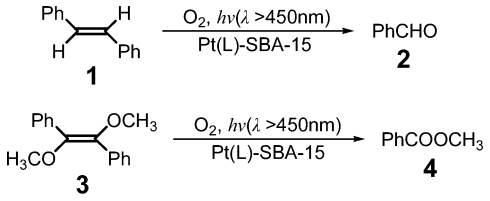

Scheme 3

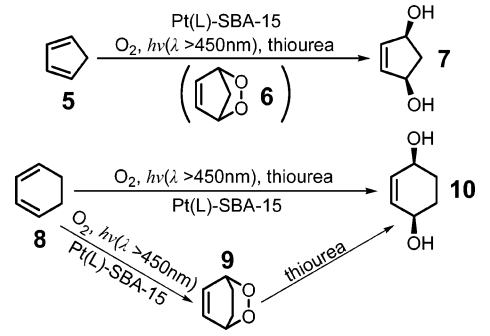

Scheme 4

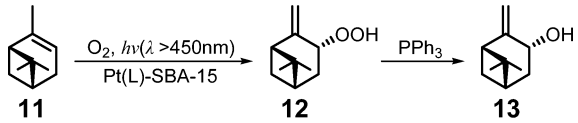

convert to their corresponding aldehyde **2** and ester **4**. The GC results indicate that the activities of the typical reactions are extremely high. Both the conversion and the yields are close to 100%.

Cyclodienes **5** and **8** undergo [4+2] cycloaddition[16] with $^1O_2$ to yield epidioxides, which can be reduced by thiourea and generate corresponding *cis*-cyclodiols **7** and **10** (Scheme 3). For either the self-polymerized dimer or the oligomers of cyclopentadiene **5** under the reaction condition, compound **7**, an important chemical for the synthesis of prostaglandins,[17] is almost the unique product obtained. Similarly, compound **10** is also the unique oxidized product of substrate **8**. The epoxy intermediate **9** can be directly observed at room temperature. ^{1}H NMR spectroscopic investigation indicates that the conversion of **8** at high concentration (0.1 M) is ~73% and the yield of **9** is 100%.

(1*S*,5*S*)-(−)-α-Pinene (**11**) takes part in an ene reaction[16] to exclusively afford **12** (Scheme 4). Following reduction by triphenyl phosphate, (1*S*,3*S*,5R)-(+)-*trans*-3-hydroxypin-2(10)-ene [(+)-trans-pinocarveol, (+)-**13**] is obtained as a unique product. The conversion is 25% monitored by GC detection.

Moreover, 7-dehydrocholesterol (**14**) is an endogenous compound of the human body, involved in a variety of biological processes. Some of its oxidation products possess potent cytotoxic and antitumor activity.[18a] As shown in Scheme 5, the photooxidation of substrate **14** affords a mixture of **15** and **16** with the molar ratio of 3:1, as directly validated from the hydrogen integral in positions 6 and 7 on the ^{1}H NMR spectrum (Figure 5), and in line with the reported value of 16:5.[18b,c] Product **15** can be separated by column chromatography on silica, while product **16** is not stable enough with such treatment. All of the above results are summarized in Table 1, and the mass balance is greater than 95%.

The efficiencies for the product formation of the above-mentioned photosensitized oxidation were investigated. Table 2 gives the quantum yields of the product formation for the photosensitized oxidation of olefin **3**. Some important features are worthy of noting based on the correlated calculation of the oxidation efficiency. In general, the process of the photosensitized oxidation involves three steps: (1) generation of $^1O_2$ by energy transfer from the triplet state of the photosensitizer to the ground state of O_2, (2) diffusion of $^1O_2$ from the generation locus to the reaction site, and (3) reaction of $^1O_2$ with the target molecule. Hence, the quantum yield (Φ) of the product formation should be the product of the quantum yield for the formation of $^1O_2$ (Φ_p), the fraction of the generated $^1O_2$ diffusing to the reaction sites (Φ_d), and the efficiency of the reaction between $^1O_2$ and the target molecules (Φ_q).

$$\Phi = \Phi_p \cdot \Phi_d \cdot \Phi_q \qquad \text{(a)}$$

The quantum yields (Φ_p) for $^1O_2$ production of SBA-15-supported photosensitizers can be determined by the 9,10-diphenylanthracence bleaching method,[19] which is around 0.40 in acetonitrile solution. The efficiency (Φ_q) for the bimolecular reaction between $^1O_2$ and target molecule can be calculated by eq b,

$$\Phi_q = k_r \cdot [Q]/(k_r \cdot [Q] + 1/\tau) \qquad \text{(b)}$$

where k_r is the reaction constant between $^1O_2$ and olefin and has the value of 1.58×10^7 mol^{-1} L s^{-1} in nonpolar solvent when we take *trans*-dimethoxystilbene (*trans*-DMOS) as the representative of the olefin.[20] τ is the lifetime of $^1O_2$ and has the value of about 36 μs in acetonitrile,[21] and [Q] is the concentration of DMOS in acetonitrile solution. As the concentration of DMOS in acetonitrile solution was 1.00×10^{-3} mol L^{-1}, Φ_q was calculated from eq b to be 0.36. The quantum yield for the product formation (Φ) was determined by the amount of product formed in the first 15 min. Using the above-obtained Φ_p and Φ_q data and the value of Φ for *trans*-DMOS in Table 2, the quantum yield for $^1O_2$ diffusion (Φ_d) was calculated to be 228% upon addition of 5 mg of platinum(II) complex-loaded SBA-15-b in acetonitrile solution. Much to our surprise, this value exceeds 100% and cannot be true. If we assume that diffusing quantum yield (Φ_d) reaches its maximum of 100%, the efficiency of Φ_q value was recalculated to be 83% in SBA-15-b (Table 2). As a result, the local concentration [Q] of DMOS should be 8.5×10^{-3} mol L^{-1}, which is 8 times higher than that in homogeneous solution (1.00×10^{-3} mol L^{-1}). This result clearly demonstrates that the olefins are remarkably enriched in the channels of SBA-15-b. As compared to our previous work in Nafion,[10a,b] the photooxidation site mainly located in the mesoporous channel inside rather than in the case of Nafion in solution outside. The quantum yield for

(17) Johnson, C. R.; Penning, T. D. *J. Am. Chem. Soc.* **1988**, *110*, 4726−4735.
(18) (a) Albro, P. W.; Bilski, P.; Corbett, J. T.; Schroeder, J. L.; Chignell, C. F. *Photochem. Photobiol.* **1997**, *66*, 316−325. (b) Albro, P. W.; Corbett, J. T.; Schroeder, J. L. *Photochem. Photobiol.* **1994**, *60*, 310−315. (c) Clennan, E. *Tetrahedron* **2000**, *56*, 9151−9179.
(19) Diwu, Z.; Lown, J. W. *J. Photochem. Photobiol., A: Chem.* **1992**, *64*, 273−287.
(20) Bartlett, P. D.; Mendenhall, G. D.; Schaap, A. P. *Ann. N.Y. Acad. Sci.* **1970**, *171*, 79−87.
(21) Frimer, A. A. *Singlet Oxygen II*; CRC Press: Boca Raton, FL, 1985; p 184.

Scheme 5

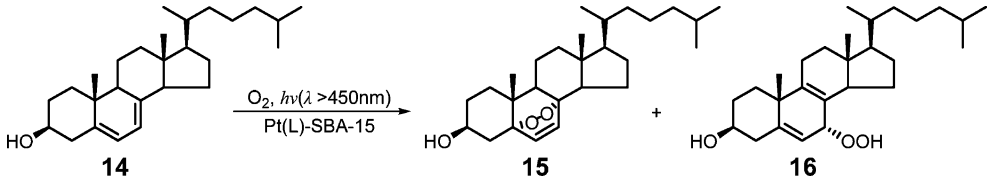

Table 1. Conversion and Yield for $^1O_2$ Photooxidation of Olefins[a]

entry	solvent	irradiation time (h)	product[h]	conv. (%)	yield (%)
1	CH_3CN	2	**2**	∼100[b]	∼100[b]
3	CH_3CN	1.1	**4**	∼100[b]	∼100[b]
5	CH_3CN	3	**7**		>95[c−e]
8	CH_3CN	3	**10**		>95[c,d]
	CH_3CN	3	**9**		>95[c,d]
	CD_3CN[g]	2	**9**	73[f]	∼100[f]
11	CH_3CN	3	**13**	25[c]	∼100[c]
14	CH_3CN	4	**15**, **16**		95[c,d]
	CD_3CN[g]	2	**15**, **16**	>95[c]	74, 26[c]

[a] Substrate/sensitizer molar ratio is about 125. [b] Concentration of the substrates is about 10^{-3} M. [c] Concentration of the substrates is about 10^{-2} M. [d] Yields are calculated on the basis of the consumption of the substrates. [e] Oligomers of cyclopentadiene are excluded. [f] Concentration of the substrates is about 10^{-1} M. [g] Tetramethylsilicane is used as the internal standard. [h] Compound **7**: MS *m*/*z* 100 (M^+), 82 $(M - 18)^+$; ^1H NMR (400 MHz, $CDCl_3$) δ 1.54 (d.t, $J = 15$ and 4 Hz, 1H), 2.70 (d.t, $J = 15$ and 7 Hz, 1H), 4.65 (d.d, $J = 7$ and 4 Hz, 2H), 6.03 (s, 2H). Compound **9**: MS *m*/*z* 112 (M^+); ^1H NMR (300 MHz, CD_3CN) δ 1.43 (br d, $J = 10$ Hz, 2H), 2.26 (br d, $J = 10$ Hz, 2H), 4.60 (br s, 2H), 6.64 (d.d, $J = 3$ and 3 Hz, 2H). Compound **10**: MS *m*/*z* 114 (M^+); ^1H NMR (400 MHz, $CDCl_3$) δ 1.74 (m, 4H), 4.09 (br s, 2H), 5.75 (s, 2H). Compound **13**: ^1H NMR (300 MHz, $CDCl_3$) δ 0.65 (s, 3H), 1.28 (s, 3H), 1.63−2.55 (m, 6H), 4.42 (d, $J = 7$ Hz., 1H), 4.82 and 5.00 (m, 2H, C═CH_2). Compound **15**: MS *m*/*z* 416 (M^+); ^1H NMR (400 MHz, CD_3CN) δ 0.80 (s, 3H, 13-CH_3), 0.90 (s, 3H, 10-CH_3), 3.71 (m, 1H, 3α-H), 6.21 (d, $J = 8.5$ Hz, 1H, 6-H) and 6.47 (d, $J = 8.5$ Hz, 1H, 7-H). Compound **16**: MS *m*/*z* 416 (M^+); ^1H NMR (400 MHz, CD_3CN) δ 0.66 (s, 3H, 18-CH_3), 3.45 (m, 1H, 3α-H), 4.55 (bs, 1H, 7-H), 5.66 (d, 1H, 6-H), 8.88 (s, 1H, 7-peroxide-H).

the product formation in this established photooxidation system is more than 100 times higher than that of Nafion case. Mesoporous molecular sieve SBA-15-b acts as not only a support for the sensitizer, but also a nano-reactor to facilitate the photooxidation.

To determine whether the supporting matrix would affect the photosensitized oxidation, mesoporous silica materials with different pore sizes were used to perform the reaction. MCM-41 and commercial silica gel were also chosen for comparison. When mesoporous silica MCM-41 with small pore size (∼2.4 nm) and similar 2-D hexagonal channel structure as SBA-15 was used as the supporting matrix, a low enriched effect was observed. This may arise from the difficulty for both the substrate and the product to enter and escape from the small channels. As compared to MCM-41, SBA-15 with larger pore size shows a higher enriched effect. The larger the pore size is, the higher the efficiency will be (Table 2, entry SBA-15-a,b). When the pore size is large enough (>6.2 nm) for the interphase mobility of the substrates and products, the decrease of the enriched effect is observed, which is possibly due to the decrease of the surface area (Table 2, entry SBA-15-c−e). However, for the silica gel, which has very large mesopore size (∼13 nm), the disordered and widely distributed pore size and low surface area result in low reaction efficiency. With respect to the correlations of the oxidation efficiency shown in Table 2, the influence of the pore size and surface area of the mesoporous molecular sieves is indeed important. The ordered mesoporous molecular sieve with high surface area and pore size larger than 6 nm was a prerequisite in this photooxidation system.

On the basis of the above results, it could be speculated that the photooxidation involves two phases: one is the homogeneous solution outside and the other is the inside channels of the SBA-15, as simulated in Scheme 1. When mesoporous SBA-15 is presented in the system, a concentration gradient of the substrate between the two phases forms before irradiation. As the irradiation goes on, the oxidized product is generated gradually and also forms a concentration gradient between the mesopores and solution. The intrinsic driving force of concentration gradient between the two phases keeps the voluntary exchange of the substrate and product until all of the substrate has been consumed. The local concentration of the substrate is more than 8 times higher than that in a homogeneous solution as diffusion quantum yield of singlet oxygen ($^1O_2$) is assumed to be unit. It must be pointed out that this is an average value and in reality it should be even larger. Importantly, this enriched effect is interrelated with the pore size and surface area of the mesoporous molecular sieves. Higher local concentration in mesoporous silicate SBA-15 affords higher quantum yield of products formation. As a result, the rate of photosensitized oxidation is greatly improved.

For kinetic and repeat experiments (Figure 6), *trans*-DMOS was selected for monitoring convenience. Time line monitoring reveals that the photooxidation is completed in about 1 h when 5 mg of platinum(II) complex-loaded SBA-15-b is employed. Unlike the organic photosensitizer-immobilized heterogeneous system, no obvious bleaching was observed. After 10 runs, there is no significant efficiency decrement of the sensitizer and almost no leaching was observed in the reaction vessel. As expected, the platinum(II) complex loaded in the channel of SBA-15 is very stable and the photosensitized oxidation occurs efficiently. The separation and recycle are realized by simple filtration in this versatile system.

Conclusion

We demonstrate that cyclometalated platinum(II) complex can be easily anchored into the pore channels of the ordered mesoporous silica SBA-15 by virtue of coordinative interaction, resulting in a versatile photosensitized oxidation system under oxygen. The efficiency of photosensitized oxidation is upgraded 100 times greater than the previous work in Nafion. Studies on the $^1O_2$ generation provide unambiguous evidence that the olefins in the nano-channels of SBA-15 can be enriched 8 times higher than that in the homogeneous one. The large pore hexagonal channel of SBA-15 is very promising as a nano-reactor for photooxidation. No obvious degradation and leaching of photosensitizers are observed after 10 runs. Only a simple filtration is needed for recycled use of the expensive noble metal catalysts. Further studies are performed to extend the scope of such nano-reactor system.

Table 2. Physicochemical Property of Silica Materials and Quantum Yields for Photosensitized Oxidation of Substrate **3**[a]

entry	pore size (nm)[b]	surface area (m^2/g)[b]	Φ[c] (%)	Φ_p[d] (%)	Φ_d (%)	Φ_q (%)	[Q] (mol L^{-1})	enriched rate
Pt(L)Cl			30	94		36	1.00×10^{-3}	
MCM-41	2.4	963	20	40	138	36	1.00×10^{-3}	1.8
						50	1.77×10^{-3}	
SBA-15-a	5.8	638	26	40	181	36	1.00×10^{-3}	3.4
						66	3.36×10^{-3}	
SBA-15-b	6.2	832	33	40	228	36	1.00×10^{-3}	8.5
						83	8.50×10^{-3}	
SBA-15-c	6.8	766	32	40	223	36	1.00×10^{-3}	7.5
						81	7.50×10^{-3}	
SBA-15-d	7.4	620	31	40	218	36	1.00×10^{-3}	6.6
						79	6.60×10^{-2}	
SBA-15-e	8.0	589	31	40	211	36	1.00×10^{-3}	5.7
						77	5.73×10^{-3}	
silica gel	13[e]	330	27	40	185	36	1.00×10^{-3}	3.6
						67	3.62×10^{-3}	

[a] Loading amount of platinum(II) complex in mesoporous molecular sieves is 0.41 wt %. [b] The values were measured before immobilization experiments. [c] The values depended on the luminous flux and the oxidation results in the first 15 min. [d] The values were determined by the 9,10-diphenylanthrancene bleaching method. [e] The value was based on statistical average.

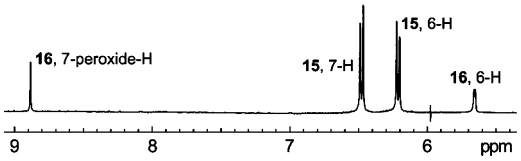

Figure 5. ^{1}H NMR spectrum of substrate **14** oxidation; the ratio of products **15** to **16** was determined by the hydrogen integral in positions 6 and 7.

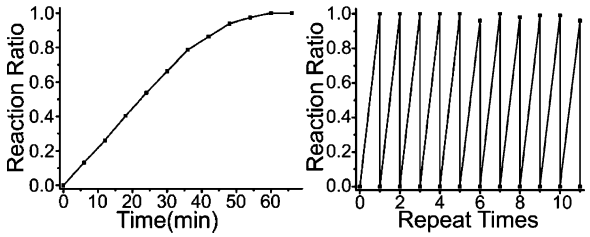

Figure 6. Kinetic plot and repeating reaction of substrate **3** in platinum-(II) complex-loaded SBA-15-b.

Experimental Section

Materials. All solvents and olefin substrates used in the reactions are analytical grade and used as received. The complex Pt(L)Cl was prepared according to the literature method.[14] The mesoporous molecular sieves (SBA-15) were prepared by using triblock copolymer P123 (Pluronic 123, $EO_{20}PO_{70}EO_{20}$) as a structure-directing agent under acidic condition at 40 °C but with different hydrothermal time and temperature as reported in the literature.[11d,e] MCM-41 was prepared by using cationic surfactant cetyltrimethylammonium bromide (CTAB) as a structure-directing agent under basic condition at 20 °C.[11c] Further modification with APTES was achieved via a refluxing process in toluene at 120 °C for 20 h. Surface covered rate could be well controlled by the different APTES/mesoporous molecular sieves ratios.

Photooxidation of Substrate and Quantum Yield Calculation. The sample in a Pyrex reactor was bubbled with oxygen during irradiation. A 500 W high-pressure Hanovia Hg lamp was employed as the light source, and a glass filter was used to cut off light with a wavelength below 450 nm. All of the quantum yields for the product formation in different pore size platinum(II) complex-loaded SBA-15 were calculated using the amount of product formed in the first 15 min of irradiation. As the generation of $^1O_2$ is a single-photon process, the corresponding luminous flux taking part in the oxidation can be determined. On the other hand, the total absorbed luminous flux can be measured by a photometer. The ratio of two luminous fluxes gave the correlated quantum yield. The quantum yield for the formation of $^1O_2$ (Φ_p) was determined by the 9,10-diphenylanthrancene bleaching method, as given in the literature.[19]

Instrumentation. Nitrogen adsorption/desorption isotherms were measured at 77 K with a Micromeritcs Tristar 3000 analyzer (USA). Before the measurements, the samples were degassed in a vacuum at 180 °C for at least 6 h. The Brunauer−Emmett−Teller (BET) method was utilized to calculate the surface areas. The pore size distributions were derived from the adsorption branches of the isotherms with use of the Barrett−Joyner−Halanda (BJH) method. UV/vis spectra were measured with a Shimadzu UV-1601PC spectrophotometer. UV-DRS spectra were measured on a JASCO UV-550. Fluorescence spectra were run on a Hitachi F-4500. Solid-state luminescent decay profiles of platinum(II) complex-loaded SBA-15 were obtained by an Edinburgh LP 920 at 547 nm using the third harmonic (355 nm) of a pulse Nd:YAG laser as the excitation resource. Gas chromatography (GC) was monitored on a Shimadzu GC-14B. ESR spectroscopic experiments were carried out at room temperature (298 K) with a Bruker ESP 300E spectrometer.

Acknowledgment. We are grateful for financial support from the National Science Foundation of China (Nos. 20333080, 20332040, 50473048, 20472092, 20403025, 20233030, 20373013, and 20421303), the Ministry of Science and Technology of China (Nos. 2003CB716802, 2004CB719903, 2006CB806105, 2007CB808004), and the Bureau for Basic Research of the Chinese Academy of Sciences.

Supporting Information Available: Preparation of platinum-(II) complex Pt(L)Cl; linear relationship between the Pt(L)Cl concentration and its absorbance at 440 nm in chloroform; and the emission decay curve of 3.3 wt % platinum(II) complex-loaded SBA-15 powder. This material is available free of charge via the Internet at http://pubs.acs.org.

JA0648256